16. The 12 experimental plants were arranged into four blocks of three, with three time periods. The design controls for variation caused by plant identity, location within the reserve (block), time of treatment, and carryover of effects (on visitation) from previously applied treatments [R. G. Petersen, *Design and Analysis of Experiments* (Dekker, New York, 1985)]. I used the Tukey test [J. H. Zar, *Biostatistical Analysis* (Prentice Hall, Englewood Cliffs, NJ, 1984)] to test two pairs of a priori pairwise predictions. To examine whether pollinators responded to increases in flower number, I tested the prediction C = B > A for visitation data. To examine effects on pollination success, I tested C > B = A for data on pollen receipt and dispersal.
17. The initial 5 days allowed local pollinators to adjust to the treatment. Residual effects of conditions preceding each treatment were controlled for by the experimental design as well (*16*). Pollen grains and pollen tubes were measured by epifluorescent microscopy (*8*). For a given treatment, grains and tubes were averaged over all intact stigmas and styles, respectively. Fluorescent dye has been used successfully to mimic relative pollen movement [S. N. Handel, in *Pollination Biology*, L. Real, Ed. (Academic Press, Orlando, FL, 1983), p. 163; N. M. Waser, *Funct. Ecol.* 2, 41 (1988)]. Twenty-four hours after dye application, I collected stigmas of all female-phase flowers on conspecific plants within 20 m, a sufficient distance to detect most dye movement from other flowers pollinated by *Lampornis calolaema* [Y. B. Linhart, W. H. Busby, J. H. Beach, P. Feinsinger, *Evolution* **41**, 679 (1987)].
18. Pollen dispersal was estimated in two ways: the median number of dye particles reaching stigmas of "visited" neighborhood flowers (those receiving at least one dye particle) and the total number of dye particles on these stigmas.
19. I could not assess treatment effects on seed production because many fruits aborted. This was partly an artifact of limiting pollen receipt to 1 day, substantially less than a natural exposure of 3 to 4 days.
20. Recently captured male hummingbirds (*L. calolaema*), the sole pollinator for *B. triflora* (*11*), were used in experiments. Details on the training and handling of birds are given in (*8*).
21. A simple model (*11*) suggests that a larger floral display will improve outcross pollen receipt per flower only if greater visitation compensates for the increased dilution of pollen among flowers. This experiment tested one assumption of the model: staminate flowers would dilute pollen loads delivered to target flowers less than would hermaphrodite flowers.
22. The short male phase, displaced stigma, and shorter and wider corolla of staminate flowers (*8*) could reduce flower contact with pollinators, limiting pollen removal from the pollinator during visits [C. Murcia, *Ecology* **71**, 1098 (1990)]. Greater longevity on plants, despite a shorter male phase, also extends the period during which a staminate flower serves only to attract pollinators (*8*).
23. In each trial, a bird (with a cleaned bill) visited these six flowers in sequence. Experimental flowers were either both hermaphrodite or both staminate; donor and recipient flowers were hermaphrodite. To avoid confusing the pollen source, I used experimental flowers in which the male phase had ended. Four trials were run for each treatment with each of six birds (n = 24 runs per treatment). After each trial, stigmas of all experimental and recipient flowers were treated (*8*) and viewed under epifluoresence to count pollen grains.
24. Because *B. triflora* exhibits strong inbreeding depression (R. Podolsky, unpublished data), plants could also benefit by avoiding increased within-plant pollination that would result from the addition of hermaphrodite flowers, which have an extended period of pollen dispersal (*8*).
25. L. A. Real and B. J. Rathcke, *Ecology* **72**, 149 (1991); M. Zimmerman and G. H. Pyke, *Am. Nat.* **131**, 723 (1988).
26. E. W. Stiles, *Am. Nat.* **120**, 500 (1982).
27. D. W. Schemske and C. C. Horvitz, *Science* **225**, 519 (1984).
28. Large maternal investment in fruits and seeds suggests that allocation to attractive tissue is chiefly paternal, which has prompted the argument that increased pollinator attraction should benefit pollen dispersal rather than pollen receipt (*3, 4*).
29. D. R. Campbell, *Am. J. Bot.* **76**, 730 (1989).
30. I thank R. Simons and M. Guindon for research assistance. D. Schemske, R. Huey, P. Feinsinger, M. Groom, and J. Kingsolver edited the manuscript. Support was provided by the National Science Foundation (NSF) (graduate fellowship), the University of Florida (presidential graduate fellowship), Sigma Xi, the Organization for Tropical Studies (Jessie Smith Noyes Foundation), and NSF grant BSR-8605043 to P. Feinsinger.

13 April 1992; accepted 4 August 1992

Middle Tertiary Volcanism During Ridge-Trench Interactions in Western California

Ronald B. Cole and Asish R. Basu*

Bimodal volcanism in the Santa Maria Province of west-central California occurred when segments of the East Pacific Rise interacted with a subduction zone along the California margin during the Early Miocene (about 17 million years ago). Isotopic compositions of neodymium and strontium as well as trace-element data indicate that these volcanic rocks were derived from a depleted-mantle (mid-ocean ridge basalt) source. After ridge-trench interactions, the depleted-mantle reservoir was juxtaposed beneath the continental margin and was erupted to form basalts. It also assimilated and partially melted local Jurassic-Cretaceous sedimentary and metasedimentary basement rocks to form rhyolites and dacites.

The middle Tertiary geologic history of western California was largely influenced by tectonic events that occurred when segments of the East Pacific Rise interacted with a subduction zone along western North America (Fig. 1). This interaction resulted in the development of the San Andreas fault system (*1*). Coeval with the ridge-trench interactions were episodes of near-trench volcanism and localized development of sedimentary basins (*1–3*). Ridge-trench interactions can be important events in the geological evolution of continental margins (*4–11*). They can also invoke geologic responses such as near-trench volcanism that are in marked contrast to typical subduction processes. Isotopic and geochemical compositions of such near-trench volcanic rocks can provide important information on the magmatic and tectonic processes that take place when a spreading ridge encounters a continental margin. Several studies on volcanic rocks in western California (*12–14*) have suggested a possible relation between mid-ocean ridge magmas and near-trench volcanic activity. However, these studies either lack a combination of isotopic petrogenetic indicators (for example, combined Nd and Sr isotopic data) or do not contain sufficient data to define a mid-ocean ridge basalt (MORB) end-member composition. In this report we describe Nd and Sr isotopic data that indicate that early Miocene volcanism in the Santa Maria Province (SMP) of west-central California was a direct result of ridge-trench interactions.

The SMP is located along onshore and offshore west-central California. Onshore it is bound by the Nacimiento and Rinconada faults to the east and north, the Santa Ynez fault to the south, and the coastline to the west (Fig. 2) (*15*). We studied tuff and basalt in the Obispo Formation and tuff in the Lospe Formation, the Tranquillon volcanic rocks, the Catway basalt, and the Lopez Mountain basalt (Fig. 2). The SMP volcanic rocks are bimodal and include basalts and basaltic andesites with rhyolites and dacites. Ages of eruption of the SMP volcanic rocks are mostly between 16 and 18 million years ago (Ma) (*16*). Available seismic and well-log data for the onshore and offshore SMP reveal that lower Miocene volcanic rocks are volumetrically significant and thicken into normal-fault–bounded basins (*17*). The short age span and the similar stratigraphic positions occupied by these volcanic rocks (*18*) suggest that they were erupted rapidly along the continental margin in close association with crustal extension and basin development.

Immediately before Santa Maria volcanism, ~19 Ma, segments of the East Pacific Rise between the Pioneer and Murray fracture zones intersected the continental margin (Fig. 1) near the paleolatitude of the SMP (*1, 19*). When segments of the East Pacific Rise intersected North America, subduction beneath the continental margin

Department of Geological Sciences, University of Rochester, Rochester, NY 14627.

*To whom correspondence should be addressed.

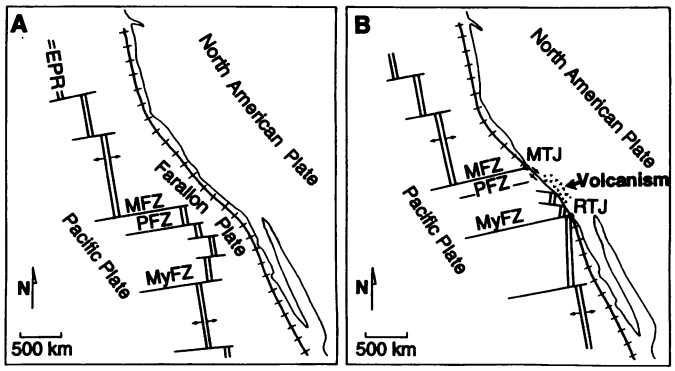

Fig. 1. Generalized Early Miocene paleogeographic reconstructions showing position of the East Pacific Rise (EPR) with respect to the North American plate at (**A**) ~35 Ma and (**B**) 20 Ma; modified from (*1, 19*). V-pattern in (B) depicts the area of Early Miocene near-trench volcanism, including the SMP. Hatched line represents the estimated position of the subduction zone along western North America. Small arrows show relative motions between adjacent plates. Present-day coastline of North America is shown for reference. MFZ, Mendocino fracture zone; PFZ, Pioneer fracture zone; MyFZ, Murray fracture zone; MTJ, Mendocino triple junction; and RTJ, Rivera triple junction. The right-lateral San Andreas fault system lies between the MTJ and RTJ and formed when the Pacific and North American plates came into contact after portions of the intervening Farallon plate were subducted (*1*).

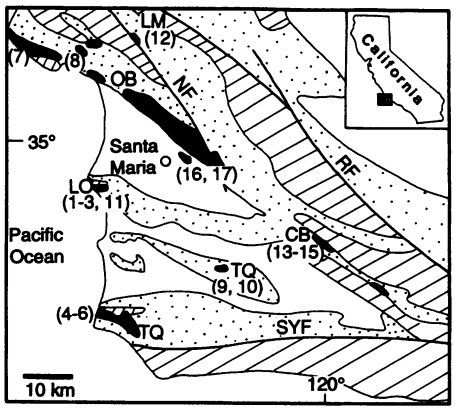

Fig. 2. Simplified geologic map of the Santa Maria Province. Black areas are outcrops of SMP volcanic rocks, stippled areas are outcrops of Eocene to Miocene sedimentary rocks, hatched areas are outcrops of Jurassic-Cretaceous Franciscan Complex, and blank areas are Pliocene and Quaternary deposits. Heavy lines are major faults. Numbers in parentheses represent locations of analyzed samples in Table 1. OB, Obispo Formation volcanic rocks; LO, Lospe Formation volcanic rocks; TQ, Tranquillon volcanic rocks; CB, Catway basalt; LM, Lopez Mountain basalt; NF, Nacimiento fault; RF, Rinconada fault; and SYF, Santa Ynez fault. Modified from (*15*).

ceased (*20*) and a transform boundary formed between the Pacific and North American plates that ultimately developed into the modern San Andreas fault system (*1*). Atwater (*1*), Dickinson and Snyder (*3*), and Severinghaus and Atwater (*19*) suggest that as segments of the East Pacific Rise approached the North American trench, the hot and buoyant young oceanic lithosphere stalled and possibly equilibrated with asthenosphere beneath the continental margin. As a result, new oceanic lithosphere was not formed when the ridge approached the trench and a no-slab region developed beneath the continental margin inboard of the ridge segments (*1, 3, 19*). The region beneath the continental margin where ridge segments interact will presumably be filled by suboceanic mantle as the preexistent oceanic plates continue to diverge after entering the subduction zone (*1, 4, 6, 19*). The accumulation of juvenile, suboceanic mantle could provide a source of magma and heat for near-trench volcanic activity in the forearc.

Our Nd-isotopic, Sr-isotopic, and major- and trace-element geochemical data (Table 1 and Figs. 3 to 5) (*21*) for the SMP bimodal volcanic rocks show that the new mantle material that had accumulated beneath the continental margin during ridge encounter was depleted and had an affinity to MORB (*22*). Santa Maria basalts exhibit $\epsilon_{Nd}(t)$ values from 8.0 to 9.3 and $^{87}Sr/^{86}Sr$ (t) values from 0.702575 to 0.704076 (Fig. 3 and Table 1). The basalts are mildly enriched in light rare-earth elements (LREE) with chondrite-normalized La/Ce ratios of 0.9 to 1.2 and Ce/Yb ratios of 1.8 to 2.6 (Table 1 and Figs. 4 and 5). The basaltic andesites and rhyolites-dacites exhibit lower $\epsilon_{Nd}(t)$ and higher $^{87}Sr/^{86}Sr$ (t) values than do the basalts (Fig. 3 and Table 1). Basaltic andesites exhibit moderate LREE enrichment with La/Ce ratios of 1.0 to 1.4 and Ce/Yb ratios of 2.2 to 3.3, and the rhyolites-dacites show greater LREE enrichment with La/Ce ratios of 1.1 to 1.4 and Ce/Yb ratios of 3.7 to 6.9 (Table 1 and Figs. 4 and 5). The above Nd- and Sr-isotopic signatures of the SMP basalts (Fig. 3) can only be attributed to a depleted mantle source and are analogous to MORB isotopic signatures from modern and relatively young oceanic spreading ridges, including the East Pacific Rise (*22, 23*). Depleted-mantle reservoirs may have existed in the subcontinental lithosphere of western North America, but volcanic rocks attributable to these sources in the western United States demonstrate relatively lower ϵ_{Nd} and higher $^{87}Sr/^{86}Sr$ compositions than do the SMP basalts (*24*). This observation suggests that the subcontinental mantle beneath the western United States was more enriched or contaminated than the source of the Santa Maria basalts and probably was not a source for Santa Maria volcanism.

The formation of the SMP basaltic andesites and rhyolites-dacites can be attributed to assimilation of low ϵ_{Nd} and high $^{87}Sr/^{86}Sr$ crustal rocks by a MORB-like magma and accompanying fractional crystallization. In $\epsilon_{Nd}(t)-^{87}Sr/^{86}Sr$ (t) space (Fig. 3), the Santa Maria volcanic rocks lie along a hyperbolic mixing trend between MORB and the range of isotopic compositions expected for local basement. The basement beneath the SMP consists of Jurassic and Cretaceous metagraywackes and

Table 1. Nd-Sr isotopic data and selected petrogenetic parameters for the 17-Ma Santa Maria Province volcanic rocks.

Sample*	$^{87}Rb/^{86}Sr$	$^{87}Sr/^{86}Sr$†	$^{147}Sm/^{144}Nd$	$^{143}Nd/^{144}Nd$†	$\epsilon_{Nd}(t)$	Ce/Yb‡
1	1.735	0.708452	0.259	0.512561	−1.63	6.94
2	1.049	0.708301	0.095	0.512501	−2.45	6.14
3	0.404	0.708525	0.125	0.512466	−3.19	4.80
4	8.279	0.710617	0.114	0.512738	+2.14	4.99
5	13.619	0.710729	0.145	0.512727	+1.85	3.83
6	2.938	0.712017	0.119	0.512759	+2.53	5.10
7	2.929	0.705386	0.141	0.512954	+6.29	3.71
8	1.065	0.706884	0.141	0.512783	+2.96	3.33
9	0.534	0.704033	0.144	0.512867	+4.59	2.62
10	0.560	0.704125	0.157	0.512943	+6.04	2.21
11	0.084	0.703659	0.236	0.513053	+8.02	2.00
12	0.082	0.704096	0.163	0.512940	+5.97	2.27
13	0.052	0.702620	0.156	0.513103	+9.16	1.98
14	0.060	0.702590	0.183	0.513114	+9.32	1.88
15	0.059	0.702615	0.172	0.513061	+8.31	1.79
16	0.091	0.703236	0.178	0.513068	+8.44	2.59
17	0.095	0.703059	0.144	0.513083	+8.80	2.21

*Samples 1 to 7 are rhyolites and dacites, 8 to 10 are basaltic andesites, and 11 to 17 are basalts. †Measured (present-day) isotopic ratios. ‡Chondrite-normalized concentrations derived from chondritic values in (*23*).

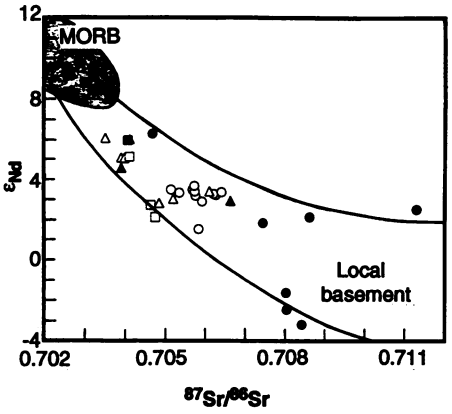

Fig. 3. Plot of initial ϵ_{Nd} and initial ($^{87}Sr/^{86}Sr$) for the SMP volcanic rocks of this study (filled symbols) and for volcanic rocks in the Tecuya Formation (open symbols) (*12*). Squares represent basalts, triangles represent basaltic andesites, and circles represent rhyolites and dacites. Notice the hyperbolic mixing relation between the basalts of the MORB field and the rhyolites and dacites through the basaltic andesites. The rhyolites-dacites plot near the "local basement," which may be defined on the basis of available data on Franciscan graywacke and metagraywacke, Great Valley sandstones, and the Sierra Nevadan Arc (*26*). The Santa Maria basalts fall in the field of MORB, which includes the East Pacific Rise. The Santa Maria samples define the end-member compositions for mixing between MORB and local crust. The Tecuya volcanic rocks also fall in this mixing field and were thought to have formed from MORB magmas as a result of ridge-trench collisions before Santa Maria volcanism 21 to 24 Ma (*12*). MORB field compiled from various sources (*22, 23*).

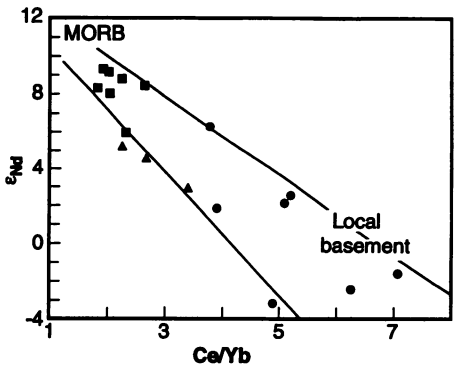

Fig. 5. Plot of $\epsilon_{Nd}(t)$ and chondrite-normalized Ce/Yb ratios for Santa Maria volcanic rocks. The linear relation among the data points suggests mixing between a MORB source and the local continental crust by assimilation-fractional crystallization processes. Rock symbols as in Fig. 3.

graywackes, Mesozoic Franciscan Complex, and small, discontinuous pods of Coast Range ophiolite (*25*). The sedimentary and metasedimentary rocks, which are also found as blocks in the Franciscan Complex, are petrographically similar to the Great Valley Group sandstones and have been interpreted as similar forearc deposits (*25*). The overall isotopic composition of the Great Valley rocks is similar to that of the Sierra Nevada arc, which shows low $\epsilon_{Nd}(t)$ and high $^{87}Sr/^{86}Sr$ (t) values (*26*). The SMP dacites and rhyolites exhibit low $\epsilon_{Nd}(t)$ and high $^{87}Sr/^{86}Sr$ (t) ratios, similar to the values expected for local sedimentary and metasedimentary basement rocks. Therefore, these volcanic rocks could have been produced by assimilation and melting of this basement by the SMP basalts. Greater enrichment of the LREE in the Santa Maria rhyolites and dacites compared to that in the basalts and basaltic andesites (Fig. 4) indicates that the basalts were contaminated by enriched local basement. Fractional crystallization, particularly of plagioclase crystals, may have contributed in part to the observed patterns of rare-earth elements in the SMP volcanic rocks (Fig. 4). The change in Eu anomaly from slightly positive and slightly negative in the basalts to a strong negative anomaly in the rhyolites and dacites is consistent with this notion (*27*). However, simple closed-system fractional crystallization of the basalts to form the basaltic andesites and rhyolites-dacites can be ruled out. This process is impossible because of the systematic decrease in $\epsilon_{Nd}(t)$ corresponding to the increases in the $^{87}Sr/^{86}Sr$ (t) and Ce/Yb ratios (Figs. 3 and 5). These observed systematic relations among the Nd- and Sr-isotopic compositions and the trace-elemental patterns of the bimodal suite strongly indicate that assimilation fractional crystallization processes were important in the evolution of these rocks.

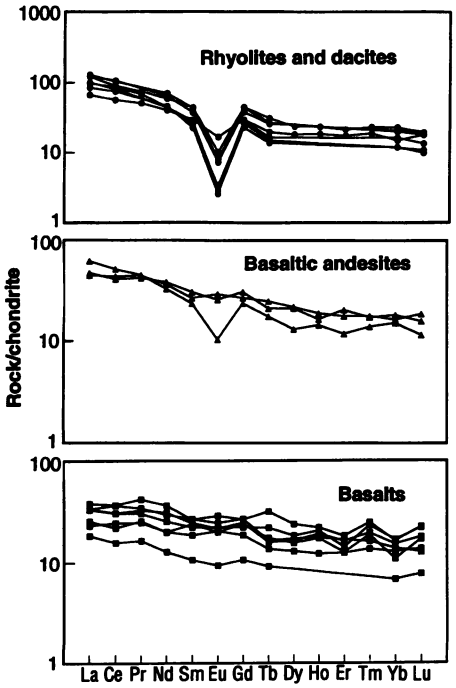

Fig. 4. Chondrite-normalized patterns of rare-earth elements for the Santa Maria volcanic rocks. Basalts show a relatively flat trend but with a slight enrichment of light rare-earth elements, compared to normal, N-type, depleted MORB (*22*). Rhyolites and dacites show marked fractionation with a negative Eu anomaly (*27*). The basaltic andesites are intermediate between the basalts and rhyolites. Rock symbols as in Fig. 3.

The isotopic and trace-element geochemical data for the SMP volcanic rocks provide strong evidence that a MORB source of magma was located beneath the early Miocene western margin of California when segments of the East Pacific Rise intersected the continental margin. These results substantiate earlier studies of other volcanic suites in western California (*12–14*; Fig. 3). They also support studies along other ancient continental subduction zones (*4, 5, 8, 10, 11*) that suggest that near-trench volcanism was related to ridge-trench interactions. The isotopic data indicate that subcontinental lithosphere was not an important magmatic source for the SMP basalts. Magmas produced from the subcontinental lithosphere would have lower $\epsilon_{Nd}(t)$ and higher $^{87}Sr/^{86}Sr$ (t) values than the Santa Maria basalts. No geochemical evidence for the presence of subcontinental lithospheric mantle beneath western California during the early Miocene has been found. This absence suggests that subcontinental lithosphere either was never present beneath the SMP or was stripped away by buoyant oceanic crust as the East Pacific Rise approached the North American trench (*1, 19*). Subsequent juxtaposition of suboceanic (depleted) mantle beneath the continental margin provided a source of MORB for volcanism in the near-trench zone. Magmas probably rose along steep-dipping trans-tensional faults that were active when the SMP experienced early Miocene clockwise rotation and crustal extension (*28*). The data presented in this report confirm that mid-ocean ridge and trench interactions provided a unique tectonomagmatic setting for plate-margin volcanism in California.

REFERENCES AND NOTES

1. T. M. Atwater, *Geol. Soc. Am. Bull.* **81**, 3519 (1970); in *The Eastern Pacific Ocean and Hawaii*, E. L. Winterer, D. M. Hussong, R. W. Decker, Eds., vol. N of *Decade of North American Geology* (Geological Society of America, Denver, CO, 1989), pp. 21–72.
2. M. C. Blake, Jr., *et al.*, *Am. Assoc. Petrol. Geol. Bull.* **62**, 344 (1978).
3. W. S. Snyder, W. R. Dickinson, M. L. Silberman, *Earth Planet. Sci. Lett.* **32**, 91 (1976); W. R. Dickinson and W. S. Snyder, *J. Geophys. Res.* **84**, 561 (1979).
4. S. Uyeda and A. Miyashiro, *Geol. Soc. Am. Bull.* **85**, 1159 (1974).
5. R. S. Marshak and D. E. Karig, *Geology* **5**, 233 (1977).

6. S. E. DeLong, P. J. Fox, F. W. McDowell, *Geol. Soc. Am. Bull.* **89**, 83 (1978).
7. S. E. DeLong, W. M. Schwarz, R. N. Anderson, *Earth Planet. Sci. Lett.* **44**, 239 (1979).
8. J. C. Moore *et al.*, *Tectonics* **2**, 265 (1983).
9. R. D. Forsythe and E. P. Nelson, *ibid.* **4**, 477 (1985).
10. R. D. Forsythe *et al.*, *Geology* **14**, 23 (1986).
11. J. P. Hibbard and D. E. Karig, *Tectonics* **9**, 207 (1990).
12. M. Sharma, A. R. Basu, R. B. Cole, P. G. DeCelles, *Conrib. Mineral. Petrol.* **109**, 159 (1991).
13. C. M. Johnson and J. R. O'Neil, *Earth Planet. Sci. Lett.* **71**, 241 (1984).
14. J. W. Hawkins and A. F. Divis, *Geol. Soc. Am. Abstr. Programs* **7**, 323 (1975); R. W. Hurst, *Geology* **10**, 267 (1982).
15. C. W. Jennings, *California Geological Data Map Series Map No. 2* (1977).
16. D. L. Turner, *Geol. Soc. Am. Spec. Pap.* **124**, 91 (1970); R. G. Stanley *et al.*, *Am. Assoc. Petrol. Geol. Bull.* **75**, 382 (1991). The bimodal classification of the SMP volcanic rocks is based on variations of total alkalies versus SiO_2 [M. J. LeBas *et al.*, *J. Petrol.* **27**, 745 (1984)].
17. D. S. McCulloch, in *The Eastern Pacific Ocean and Hawaii*, E. L. Winterer, D. M. Hussong, R. W. Decker, Eds., vol. N of *Decade of North American Geology* (Geological Society of America, Denver, CO, 1989), pp. 439–470; K. D. McIntosh, D. L. Reed, E. A. Silver, A. S. Meltzer, *J. Geophys. Res.* **96**, 6459 (1991); A. S. Meltzer and A. R. Levander, *ibid.*, p. 6475.
18. C. A. Hall, Jr., *J. Geophys. Res.* **86**, 1015 (1981); R. B. Cole, R. G. Stanley, A. R. Basu, *Geol. Soc. Am. Abstr. Programs* **23**, A476 (1991).
19. J. Severinghaus and T. Atwater, *Geol. Soc. Am. Mem.* **176**, 1 (1990).
20. The behavior of a spreading ridge as it interacts with a continental subduction zone depends primarily on the relative velocities of plates and the angle of intersection between the ridge and the trench (*1, 3–5, 7*). In some cases, when spreading ridges are oriented at high angles (nearly perpendicular) to a trench, such as possibly occurred along the Aleutian and Japanese trenches, subduction of oceanic lithosphere resumed after apparent ridge subduction (*4, 11*).
21. Concentrations of Rb, Sr, Sm, and Nd and all the other rare-earth elements were determined by inductively coupled plasma mass spectroscopy in aqueous solutions of the rock samples, with internal standards and verification of results against rock standards such as BCR-1. Errors in these analyses are usually ±2%. Analytical clean laboratory procedures and mass spectrometric techniques for Sr- and Nd-isotopic measurements are similar to those reported in A. R. Basu *et al.* [(*Earth Planet. Sci. Lett.* **100**, 1 (1990)]. The notation $\epsilon_{Nd}(t)$ refers to 0.1-mil deviations of $^{143}Nd/^{144}Nd$ from bulk earth calculated at 17 Ma with standard parameters. Errors in the Sr- and Nd-isotopic ratio measurements are usually ±30 and ±15, corresponding to the last two digits, respectively.
22. Studies with Nd, Sr, and Pb isotopes of MORBs have characterized their mantle sources by a remarkably coherent set of parameters. For example, MORB typically exhibits $^{87}Sr/^{86}Sr$ between 0.7024 and 0.7032 and ϵ_{Nd} between +8.0 and +11.0. C. J. Allegre, B. Hamelin, B. Dupre, *Earth Planet. Sci. Lett.* **71**, 71 (1984); R. S. Cohen and R. K. O'Nions, *J. Petrol.* **23**, 299 (1982); B. Hamelin, B. Dupre, C. J. Allegre, *Earth Planet. Sci. Lett.* **76**, 288 (1986); J.-G. Schilling, *Nature* **314**, 62 (1985); M. Wilson, *Igneous Petrogenesis* (Unwin Hyman, London, 1989).
23. S.-S. Sun, R. W. Nesbitt, A. Y. Sharaskin, *Earth Planet. Sci. Lett.* **44**, 119 (1979); S. R. Taylor and S. M. McLennan, *The Continental Crust: Its Composition and Evolution* (Blackwell, Oxford, 1985); S.-S. Sun and W. F. McDonough, in *Magmatism in the Ocean Basins*, A. D. Saunders and M. J. Norry, Eds. (Blackwell, Oxford, 1989), pp. 313–345.
24. J. G. Fitton, D. James, P. D. Kempton, D. S. Ormerod, W. P. Leeman, in special volume of *J. Petrol.* on Oceanic and Continental Lithosphere (1988), p. 331; F. V. Perry, W. S. Baldridge, D. J. DePaolo, *J. Geophys. Res.* **92**, 9193 (1987).
25. W. R. Dickinson, R. V. Ingersoll, D. S. Cowan, K. P. Helmold, C. A. Suczek, *Geol. Soc. Am. Bull.* **93**, 95 (1982); H. McLean, *U.S. Geol. Surv. Bull.* **1995-B**, B1 (1991).
26. Z. E. Peterman, C. E. Hedge, R. G. Coleman, P. D. Snavely, Jr., *Earth Planet. Sci. Lett.* **2**, 433 (1967); D. J. DePaolo, *J. Geophys. Res.* **86**, 10470 (1981); A. M. Linn, D. J. DePaolo, R. V. Ingersoll, *Geology* **19**, 803 (1991).
27. Abnormal Eu enrichment relative to Sm and Gd (atomic numbers 62 and 64, respectively), on either side of it, is referred to as a positive Eu anomaly; depletion is a negative Eu anomaly. Europium is preferentially retained in the feldspars relative to surrounding rare-earth elements, so that a negative anomaly results in the residual melt. A positive anomaly suggests feldspar accumulation and a negative anomaly indicates feldspar fractionation.
28. J. S. Hornafius, B. P. Luyendyk, R. R. Terres, M. J. Kamerling, *Geol. Soc. Am. Bull.* **97**, 1476 (1986).
29. Supported by American Chemical Society grant PRF 23405-AC2 and National Science Foundation grant EAR9118008. We thank E. Wyse for the trace elemental analysis, M. Sharma for assistance in thermal ionization mass spectrometry, and P. G. DeCelles, R. G. Stanley, and R. J. Poreda for helpful discussions and early reviews. Two anonymous reviewers provided helpful reviews and comments.

8 June 1992; accepted 11 August 1992

Contribution of Oceanic Gabbros to Sea-Floor Spreading Magnetic Anomalies

Eiichi Kikawa* and Kazuhito Ozawa

The contribution of oceanic gabbros, representative rocks for layer 3 of the oceanic crust, to sea-floor spreading magnetic anomalies has been controversial because of the large variation in magnetic properties. Ocean Drilling Program (ODP) Leg 118 contains a continuous 500.7-meter section of oceanic gabbro that allows the relations between magnetization and petrologic characteristics, such as the degree of metamorphism and the magmatic evolution, to be clarified. The data suggest that oceanic gabbros, together with the effects of metamorphism and of magmatic evolution, account for a significant part of the marine magnetic anomalies.

The location of the magnetized rocks of the oceanic crust that are responsible for sea-floor spreading magnetic anomalies has been a long-standing problem in geophysics (*1–3*). The recognition of these anomalies was a keystone in the development of the theory of plate tectonics. Our present concept of oceanic crustal magnetization is much more complex than the original, uniformly magnetized model of Vine-Matthews-Morley (*1–12*). Magnetic inversion studies indicated that the upper oceanic extrusive layer (layer 2A, 0.5 km thick) was the only magnetic layer and that it was not necessary to postulate any contribution from the sheeted dike complex (layer 2B, 1.0 km) or from the intrusive layer (layer 3, 4.5 km) (*13–15*). Direct measurements of the magnetic properties of the oceanic rocks from the sea floor, however, have shown that (i) the magnetization of layer 2A is insufficient to give the required size of observed magnetic anomalies and (ii) some contribution from lower intrusive rocks is necessary (*1–3, 16*). The magnetic data of oceanic intrusive rocks have been equivocal, in part because studies were conducted on unoriented dredged and ophiolite samples and on intermittent Deep Sea Drilling Project (DSDP)/ODP cores (*1–3, 6–12*). In this study, we describe the magnetic properties of lower intrusive rocks, using the oceanic gabbros recovered during ODP Leg 118 (hole 735B at the Southwest Indian Ridge). With an extremely high recovery rate of 87%, Leg 118 gabbros may represent an excellent type section for layer 3 at this site (*17–19*).

Analysis of the rocks showed that their measured blocking temperatures were near 580°C; this value implies that the remanence is primarily carried by a low-titanium magnetite. Many of the natural remanent magnetizations (NRMs) were, however, altered: NRM inclinations were about equally divided between normal and reversed polarity, whereas all samples showed a reversed stable inclination with an average of 66° ± 5°, slightly deeper than that expected from the location of hole 735B (33°S). The unstable component of normal polarity is probably drilling-induced remanence, and the in situ magnetization may be close to the stable reversed magnetization. The stable remanence of reversed polarity (estimated average of 1.6 A/m), probably acquired during the crystallization of gabbros and

E. Kikawa, Department of Geophysics and the Geodynamics Research Institute, Texas A&M University, College Station, TX 77843–3114, and Marine Geology Department, Geological Survey of Japan, Tsukuba 305, Japan.
K. Ozawa, Department of Geology and Geophysics, Yale University, Post Office Box 6666, New Haven, CT 06511–8130, and Geological Institute, University of Tokyo, Tokyo 113, Japan.

*Present address: Marine Geology Department, Geological Survey of Japan, 1-1-3 Higashi, Tsukuba, Ibaraki 305, Japan.